



## Modeling the Propagation of Flood Waves at the Mouth of the Comoé River in Grand-Bassam (South East of Côte d'Ivoire)

Kouakou Hervé Kouassi<sup>1\*</sup>, Zilé Alex Kouadio<sup>1</sup>, Yao Alexis N'go<sup>2</sup>, Berenger Koffi<sup>1</sup> and Gla Blaise Ouédé<sup>1</sup>

<sup>1</sup>Laboratory of Science and Technology of Environment, Jean Lorougnon Guédé University, BP 150 Daloa, Côte d'Ivoire.

<sup>2</sup>Laboratory of Geosciences and Environment, UFR Environmental Science and Management, Nangui Abrogoua University, Abidjan, Côte d'Ivoire.

### Authors' contributions

This work was carried out in collaboration among all authors. Author KHK wrote the manuscript. Authors ZAK and YAN assisted in the preparation of the manuscript. Authors BK and GBO analyzed the data and KHK supervised the study. All authors read and approved the final manuscript.

### Article Information

DOI: 10.9734/IJECC/2021/v11i130328

*Editor(s):*

(1) Dr. Gamal Abdel-Hafez Mahmoud Bekhet, King Faisal University, Saudi Arabia.

*Reviewers:*

(1) John D. Fenton, Vienna University of Technology, Austria.

(2) Abeer Awad Mahmoud, Mansoura University, Egypt.

Complete Peer review History: <http://www.sdiarticle4.com/review-history/64461>

Original Research Article

Received 15 November 2020

Accepted 21 January 2021

Published 12 February 2021

### ABSTRACT

This study was carried out in order to determine the areas at risk of flooding during high water periods at the mouth of the Comoé River in Grand-Bassam. The database is essentially made up of hydro-climatic data, satellite images and topographic data. According to the various criteria, the Weibull law was selected to estimate the maximum frequency flows. According to this law, the flows at the return periods of 2, 10, 50 and 100 years are respectively 634, 733, 781 and 797 m<sup>3</sup> / s. The modeling results showed that the areas exposed to the risk of flooding are located near the Ouladine lagoon and the Ebrié lagoon at the mouth of the Comoé river. The extent of the floodplains varies with flooded areas of the order of 85.63 km<sup>2</sup>; 89.42 km<sup>2</sup>; 101.67 km<sup>2</sup>; 107.10 km<sup>2</sup> for the return periods of 2; 10; 50 and 100 years old.

*Keywords:* Propagation of flood; flood waves; flooding; natural disasters.

## 1. INTRODUCTION

The climatic variations observed in the world during these last decades have greatly influenced the water resources of the countries of the African continent. Côte d'Ivoire is not exempt from this phenomenon [1-5]. Water is a very important resource in the development of all civilizations. But its management poses problems of use, scarcity and flooding. All over the world, floods cause massive damage every year, both material and human. In most regions of the globe they cause more than 50% of natural disasters: on average 20,000 deaths / year worldwide [6].

In 2007, West African countries experienced the worst flooding in decades, resulting in loss of life and property damage [7]. Like other countries in West Africa, Côte d'Ivoire is affected by this natural disaster [8]. In particular, in the south of the country, there is a lot of damage (material goods and loss of human life) in the rainy season.

The town of Grand-Bassam, located in the south-east of Côte d'Ivoire, is not on the margins of these floods. This phenomenon is mainly caused by the closure of the mouth of the Comoé river at Grand-Bassam [9]. Indeed, the Comoé River flowed directly into the Atlantic Ocean. But, over the years, sediments have accumulated and blocked this access. This situation does not favor exchanges between the river and the ocean. Now, the river flows into the Ebrié lagoon at Grand-Bassam and creates floods during floods. This study aims to model the propagation of floods at different return periods at the mouth of the Comoé River. It will make it possible to prevent possible floods which cause loss of human life and ultimately determine the flood zones.

## 2. DATA AND METHODS

### 2.1 Data

The material used for this study consists of satellite, hydrometric and digital altitude model (DEM) data.

- The hydrometric data used during this study are those of the Yakassé-Comoé station. They relate to daily time-step flows from 1996 to 2004. They have made it possible to determine the quantiles of floods and to simulate the propagation of floods at the mouth of the Comoé River.

- A digital altitude model (DEM) of 30 m resolution for simulations at different return periods.

### 2.2 Methods

#### 2.2.1 Method for estimating flood quantiles

##### 2.2.1.1 Steps of frequency analysis

Frequency analysis is a statistical method of prediction consisting in studying past events, characteristic of a given (hydrological) process, in order to define the probabilities of future occurrence [10]. To carry it out, we used the HYFRAN (Hydrological Frequency Analysis) software developed at INRS-Water, Earth and Environment (HYDRO-QUEBEC). This program is used for checking the homogeneity of hydrological data by subjecting them to adjustments made for each of the existing laws in the HYFRAN software [11]. This step consisted of classifying chronological data in ascending order and calculating the maximum floods from the return periods of 2, 10, 50 and 100 years. Once the quantiles are estimated, these values can be used as input data to simulate the spread of floods.

#### 2.2.2 Dynamics of the water course at different return periods

##### 2.2.2.1 Flood propagation model

A 2D model is produced using HEC-RAS (Hydrologic Engineering Centers River Analysis System) software, in order to simulate floodplains for various return periods. Indeed, 2D flood maps allow a better representation and a precise quantification of the extent of flooding. This represents a decision-making tool and identification of priority areas for immediate interventions, during disaster scenarios.

For the simulation of the dynamics of the watercourse at different return periods, the hydrological parameters are not a function of time. The equations involved are:

- Equation of the conservation of mass:

$$\frac{\partial(hu)}{\partial x} + \frac{\partial(hv)}{\partial y} + q = 0 \quad (1)$$

Where:

u and v are the velocity components in the x and y directions respectively and q is a tributary flow term.

□ Continuity equation

In vector form, it takes the following form

$$\nabla \cdot (HV) + q = 0 \tag{2}$$

Where:

$V = (u, v)$ : speed vector and  $\nabla$ : vector of partial derivative operators given by

$$\nabla = \left( \frac{\partial}{\partial x}, \frac{\partial}{\partial y} \right) \tag{3}$$

2.2.2.2 Discretization of the flood propagation model

The mesh used covers the mouth of the Comoé River from upstream to the outlet at Grand-Bassam. The mesh was made on a digital model with a resolution of 90 m. In this 2D mesh, the initial 50m x 50m square cell spacing was fixed (Fig. 1).

2.2.2.3 Calibration and validation of the 2D flood propagation model

The purpose of the calibration and validation of the model is to best reproduce the behavior of the watercourse. The calibration was carried out with the flows from January 01 to December 31, 1998 (wet period) and validated with those from January 01 to December 31, 2002 (dry period). A

Manning coefficient of  $0.05 \text{ m}^{1/3} \cdot \text{s}^{-1}$  was used due to the sinuosity of the stream and the presence of vegetation [12]. The time step selected for the simulation is 2 hours. The longitudinal slope of the natural terrain ( $0.00001 \text{ m / m}$ ) is imposed as a downstream condition. The fit between the predicted and observed values was evaluated using two functions: the Nash coefficient and the correlation coefficient given respectively by equations (6) and (7). The simulation of the flow dynamics itself is made with the flows from January 1 to December 31, 2004. This period is chosen because of the extreme floods that have occurred there.

$$\text{Nash coefficient: } \text{NTD} = 1 - \frac{\sqrt{\sum_{i=1}^n (q_{ci} - q_{oi})^2}}{\sqrt{\sum_{i=1}^n (q_{oi} - \bar{q}_o)^2}} \tag{6}$$

Correlation

$$\text{Coefficient: } R = \frac{\sum_{i=1}^n (q_{ci} - \bar{q}_c) - (q_{oi} - \bar{q}_o)}{\sqrt{\sum_{i=1}^n (q_{ci} - \bar{q}_c)^2 \sum_{i=1}^n (q_{oi} - \bar{q}_o)^2}} \tag{7}$$

Where,

- $n$  represents the height of the sequence;
- $q_{oi}$  represents the flow rate observed for the time step  $i$  in  $\text{m}^3/\text{s}$ ;
- $q_{ci}$  is the flow rate calculated in  $\text{m}^3/\text{s}$  for the time step  $i$ ;
- $\bar{q}_o$  is the average flow rate observed in  $\text{m}^3/\text{s}$ .

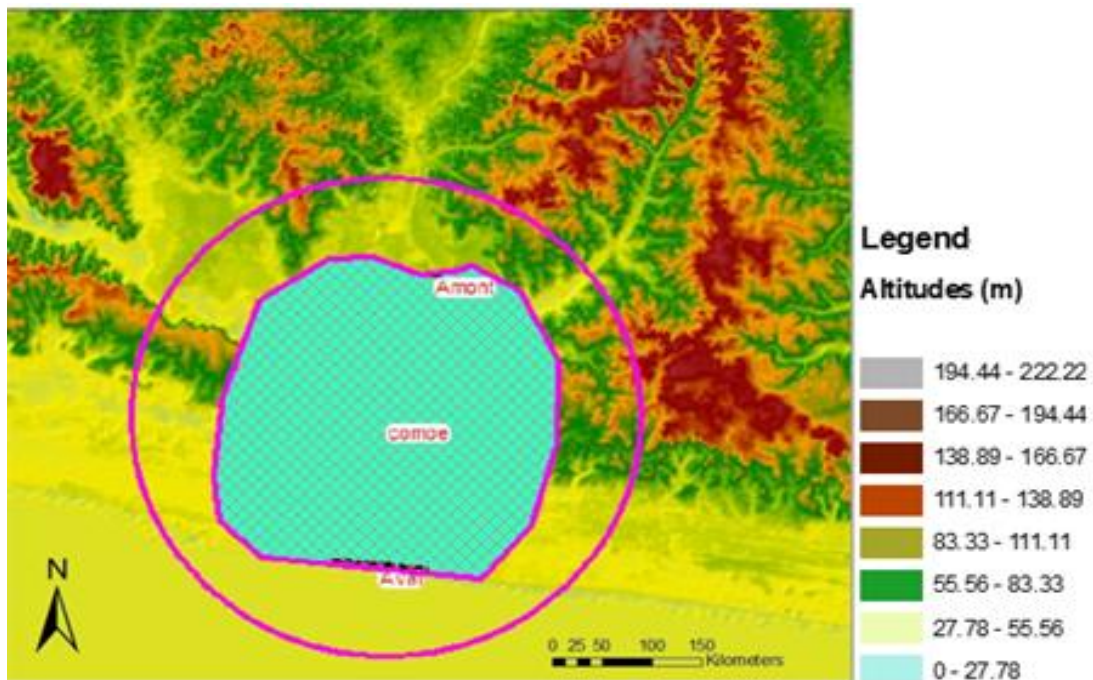


Fig. 1. Grid surface for the modeling of flood propagation

### 3. RESULTS AND DISCUSSION

#### 3.1 Flood Quantiles

The results obtained by the graphical comparison criterion are presented in Figs. 2 and 3. According to visual examination by the graphical method, the Weibull law (W2, A) has the advantage of being a simple model for this. Station whose daily flow values are well correlated with this law, which shows good behavior compared to other laws.

Table 1 presents the classification of the laws adjusted to the series of average daily flows. According to the comparison criteria, it is Weibull's law which adjusts well to the moduli of the mouth of the Comoé River then comes the Normal law, followed by the GEV law (Generalized Law of Extreme Values) and finally the Gumbel's law.

Indeed, the Akaike and Bayesian information criteria (AIC and BIC) make it possible to retain Weibull's law (Table 2). This law came first among all the laws put in competition with the greatest a posteriori probability  $P(M_i / X) = 42.8$  and the lowest values of criteria of AIC and BIC which are respectively 110.6 and 110, 2. The Normal law comes in second position with a posterior probability  $P(M_i / X) = 30.5$ , criteria values of AIC (111.3) and BIC (110.9). The GEV law comes in third position with a posterior probability value  $P(M_i / X) = 18.3$  and higher AIC (112.3) and BIC (111.7) values. Finally, Gumbel's law in last position with a low posterior probability value  $P(M_i / X) = 8.2$  and a high criterion value of AIC and BIC which are respectively 113.9 and 113.5.

The flood quantiles for various return periods are reported in Table 2. Note that the results estimated by the different laws vary very little from one return period to another. However, a significant variation is observed in the flows estimated by Gumbel's law for the return periods of 10; 50 and 100 years with respective flows of 813; 990; and 1070  $m^3/s$ . Gumbel's law tends to overestimate the flow rates.

#### 3.2 Dynamics of the Stream with Floods of Return Periods of 2; 10; 50 And 100 Years

##### 3.2.1 Results of the flood propagation model at calibration and validation

The graphs in Fig. 4 show the evolution of simulated and observed flows. Through these

graphs, we see that the model reproduces the environmental conditions well. The performance of the model is reflected by a correlation coefficient of 95% and a Nash coefficient of 72%. This strong correlation also shows that the model reproduces the hydrodynamic conditions of the medium well.

The 2002 flows used for model validation show good synchronism between the simulated and observed flows (Fig. 5). This is confirmed by the shape of the curves of variation of simulated and observed flows. The various numerical tests carried out on the measured and observed values show a good correlation of these values. This good correlation results in a correlation coefficient of 93% and a Nash coefficient of 61.10%. The numerical and graphic results show that the model reproduces the flow rates well.

##### 3.2.2 Propagation of the stream for the 2-year period

The distribution of the altitudes of the free water surface is shown by the image in Fig. 6 for the 2-year return period. It appears that the highest water levels are in the upstream part of the section of the river where the maximum can reach a height of 21.3 m. The lowest water levels (-13.8 m) are observed downstream, near the town of Grand-Bassam. The flooded area for this flood is 85.63  $km^2$ .

##### 3.2.3 Propagation of the watercourse for the period of 10 years

The distribution of the altitudes of the free water surface is shown by the image in Fig. 7 for the 10-year return period. It appears that the highest water levels are in the upstream part of the section of the river where the maximum can reach a hill of 21.4 m. The lowest water levels (-12 m) are observed downstream, near the town of Grand-Bassam. The flooded area for this flood is 89.42  $km^2$ , an increase of 4.25% compared to the return period of 2 years.

##### 3.2.4 Propagation of the watercourse for the period of 50 years

The distribution of the altitudes of the free water surface is shown by the image in Fig. 8 for the 50-year return period. It appears that the highest water levels are in the upstream part of the section of the river where the maximum can reach a hill of 21.8 m. The lowest water levels (-8.8 m) are observed downstream, near the town of Grand-Bassam. The flooded area for this flood

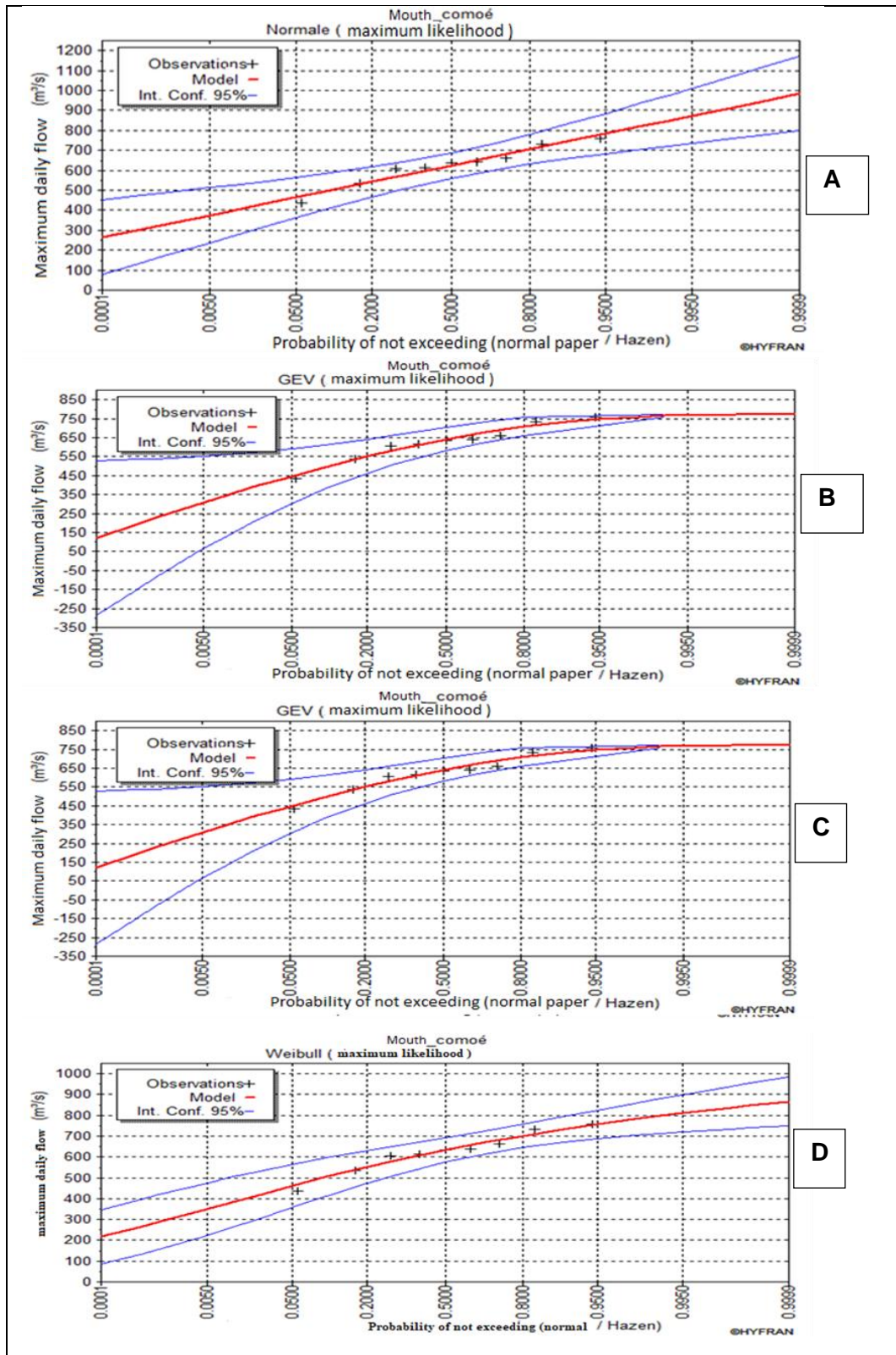


Fig. 2. Weibull (A), gumbel (B), gev (C) and normal (D) laws fitted by the maximum likelihood method to the series of annual mean flows



is 101.67 km<sup>2</sup>, an increase of 12.05% compared to the ten-year flood.

### 3.2.5 Propagation of the watercourse for the period of 100 years

The distribution of the elevations of the free water surface is shown by the image in Fig. 9 for the return period of 100 years. It appears that the highest water levels are in the upstream part of the section of the river where the maximum can reach a coast of 22.3 m, the lowest water levels (-11.9 m) are observed

downstream, near the town of Grand-Bassam. The flooded area for this cure is 107.10 km<sup>2</sup>, an increase of 5.07% over the return period of 50 years.

The result of the superposition of the flood propagation on the satellite image made it possible to observe the areas at risk of flooding at the level of the city of Grand-Bassam and its surrounding localities, according to these results, this is the period 100-year return that offers the most damage in terms of localities affected by floods.

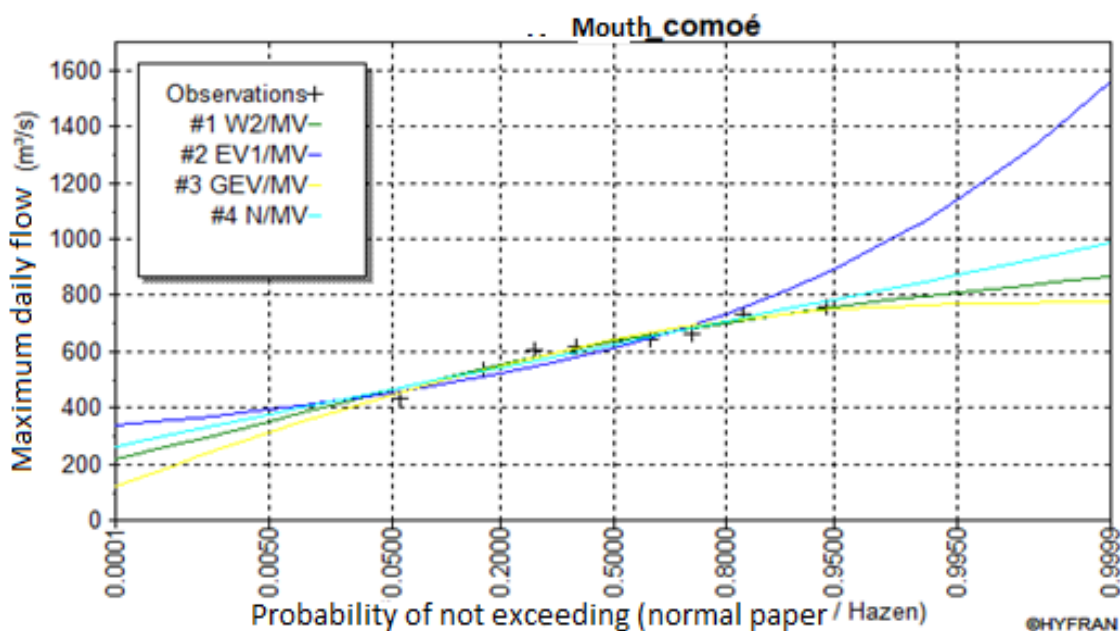


Fig. 3. Graphical comparison criterion

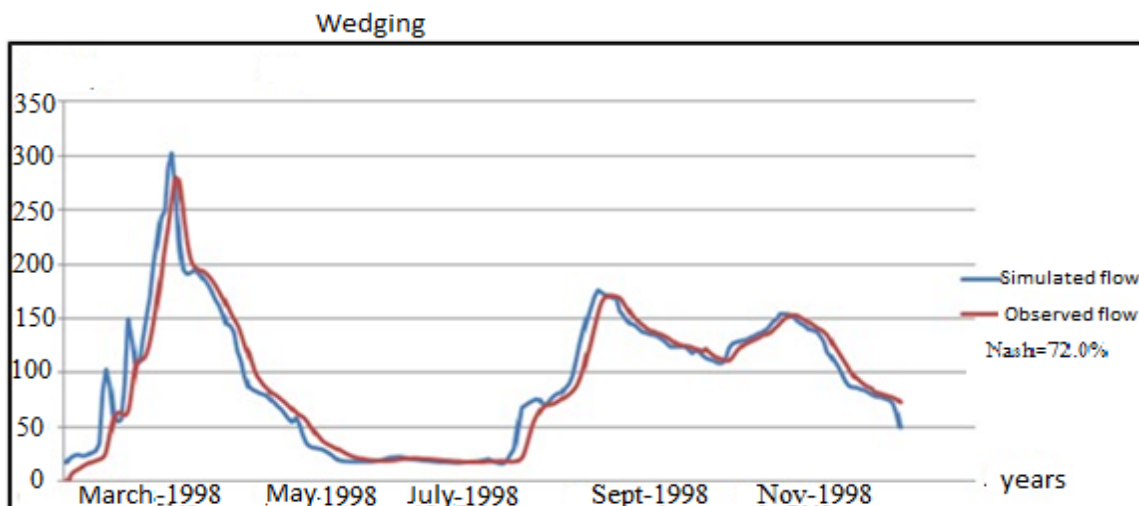


Fig. 4. Comparison of observed and simulated flows from January 01, 1998 to December 31, 1998

**Table 1. Comparison of statistical laws for the adjustment of the moduli of the mouth of the Comoé River**

Models (Maximum likelihood)	Number of parameters	Xt	P(Mi)	P (Mi/X)	Aic	Bic
Weibull	2	796,8	25	42,8	110,6	110,2
Normal	2	849,8	25	30,5	111,3	110,9
Gev	3	765,4	25	18,3	112,3	111,7
Gumbel	2	1065,1	25	8,2	113,9	113,5

**Table 2. Flood quantiles and flow return periods**

Return period (Years)	Probability of non-exceedance (Q)	Flow (M <sup>3</sup> /S) with weibull	Flow (M <sup>3</sup> /S) with NORMAL	Flow (M <sup>3</sup> /S) with gev	Flow (M <sup>3</sup> /S) with gumbel
2	0,5	634	624	641	612
10	0,9	733	749	733	813
50	0,98	781	823	760	990
100	0,99	797	850	765	1070

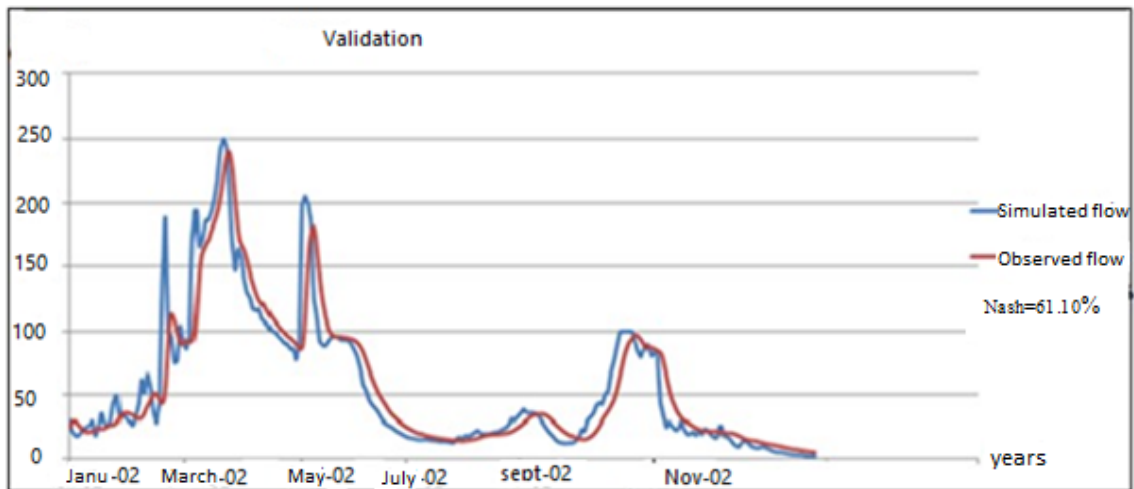


**Fig. 5. Comparison of observed and simulated flows from January 01, 2002 to December 31 2002**

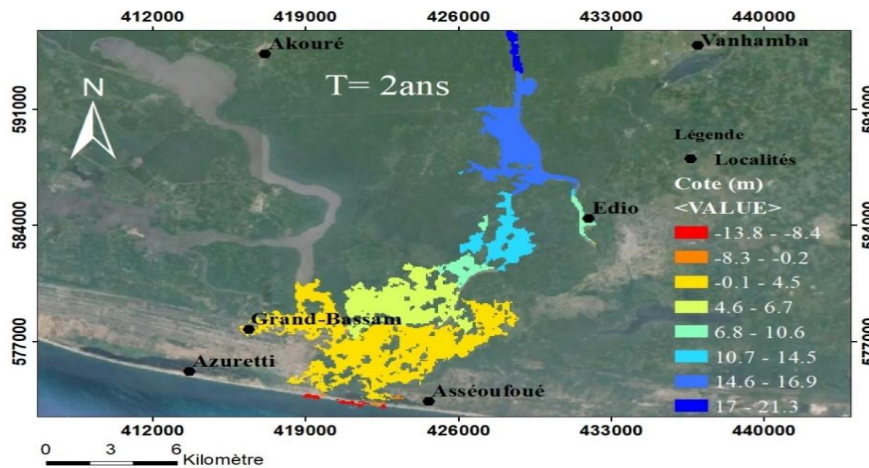


**Fig. 6. Extent of flooding of the Comoé River for the return period of 2 years**

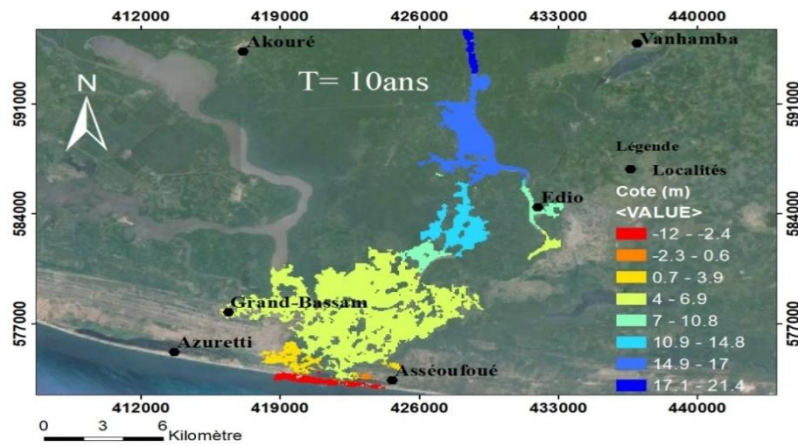


Fig. 7. Extent of flooding in the Comoé River for the 10-year return period

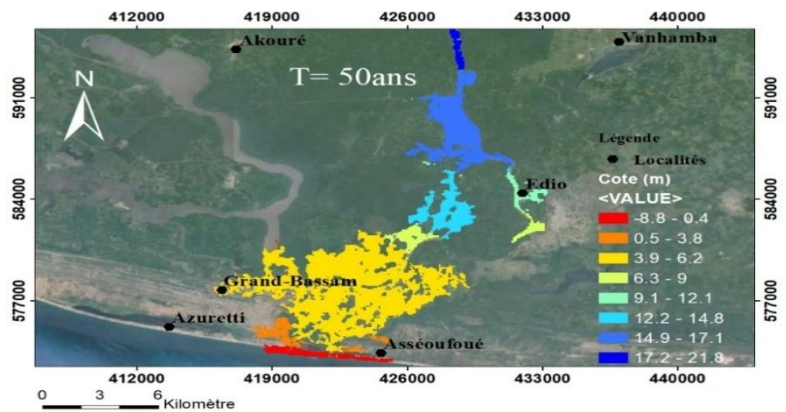


Fig. 8. Extent of flooding in the Comoé River for the 50-year return period

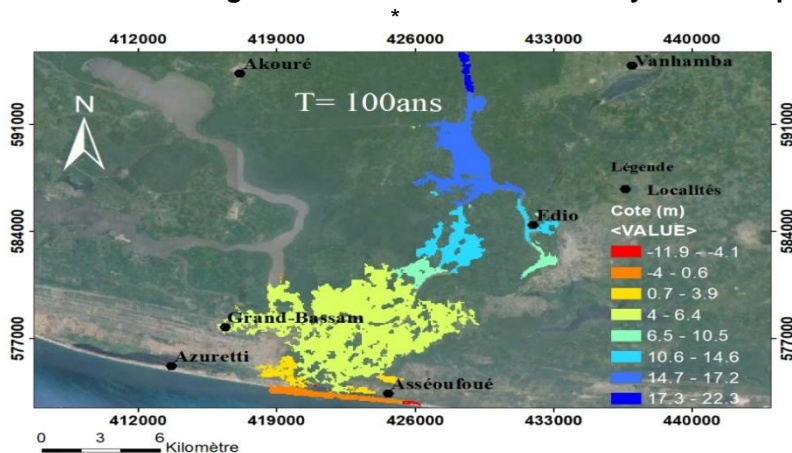


Fig. 9. Extent of flooding in the Comoé River for the return period of 100 years

#### 4. DISCUSSION

The frequency analysis carried out to estimate the flood quantiles of the Comoé River. The statistical laws applied are: Weibull's law, Gumbel's law, the normal law and GEV's law.

Based on the comparison criteria, Weibull's law best fits the moduli of the Comoé River for a 95% confidence interval because it was accepted by the various tests applied. These results are consistent with those of Soro [13] on the statistical modeling of extreme rains in Côte



d'Ivoire showing that Weibull's law fits well in the South-East of Côte d'Ivoire.

Modeling the propagation of floods to the south of the Comoé River using the HEC-RAS software has made it possible to determine the areas flooded during the flood period in the Grand-Bassam area. The Manning coefficient used for the calibration of the model is  $0.06 \text{ m}^1 / 3. \text{ s}^{-1}$ . This value is certainly large, but acceptable, due to the sinuosity of the stream and the roughness of the bed. These results confirm those of many researchers [12-16] who indicate that the Manning-Strickler coefficient is generally high for rivers with several meanders and vegetation on the banks.

The extent of the floodplains varies with free surface elevations of water from 3.5 m to 21.8 m to. In view of the results of the simulations, we can say that the city of Grand-Bassam is an area at risk of flooding for each return period. The areas that are exposed are located in the vicinity of the Ebrié lagoon and the Ouladine lagoon at the mouth. These zones concern the Mossou, Oddos, Phare, Petit-Paris, Lycée districts as well as the France district. The closure of the mouth and the change in land use are undoubtedly the cause of these flooding phenomena. Indeed, the acceleration of urbanization observed in the study area brings with it the waterproofing of soils and the creation of artificial drainage paths. This waterproofing of the soil coupled with deforestation favors the runoff of water towards the one and only mouth, the lowest point of the coast. Since the closure of this mouth, these waters no longer manage to flow into the sea and contact has been broken between the Comoé River and the said sea. The river now flows into the Ebrié lagoon and causes flooding during the floods. These results are confirmed by the work of [17] and by those of [18] in the same context of modeling the propagation of flood waves. According to these authors, any modifications to the soil (deforestation, agricultural practices, waterproofing) reduce the penetration of water into it, promote runoff and therefore water concentration, leading to an increase in the submerged perimeters and therefore a large flood area. The same observation was made by [19,20] who indicate that urbanization correlated with soil waterproofing is the basis of many floods.

## 5. CONCLUSION

This study made it possible to highlight the extent of the propagation of flood waves as well as the location of areas vulnerable to flooding. Concerning the estimation of the flood quantiles for certain return periods, Weibull's law fits well to the modules of the Comoé River with the greatest a posteriori probability 42.8 and the lowest values of criteria of BIC and AIC which are respectively 110.2 and 110.6.

The results of the simulation of the dynamics of the Comoé River at different return periods have made it possible to identify the areas that are exposed to the risk of flooding during flood periods. These are located in the vicinity of the Ouladine lagoon and the Ebrié lagoon at the mouth. Flooding can be brought under control in the study area in order to protect the city of Grand-Bassam. For future studies, it would be interesting to couple hazard and vulnerability. This will certainly allow the identification of flood risk zones with much more precision.

## COMPETING INTERESTS

Authors have declared that no competing interests exist.

## REFERENCES

1. Kouakou KE, Goula BTA, Savané I. Impacts of climate variability on surface water resources in humid tropical zones: Case of the transboundary watershed of Comoé (Côte d'Ivoire - Burkina Faso). *European Journal of Scientific Research*. 2007;16(1):31-43.
2. Koffi B, Kouadio Z., Kouassi K, Yao A, Sanchez M, Kouassi K. Impact of meteorological drought on streamflows in the Lobo River Catchment at Nibéhibé, Côte d'Ivoire. *Journal of Water Resource and Protection*. 2020;12:495-511. DOI: 10.4236/jwarp.2020.126030
3. Kouakou KE. Impacts of climate variability and climate change on water resources in West Africa: Case of the Comoé watershed. Unique Doctoral Thesis, Abobo-Adjamé University (Ivory Coast). 2011;186 .
4. Yao AB, Goula BTA, Kouadio ZA, Kouakou KE, Kane A, Sambou S. Analysis of climatic variability and quantification of water resources in humid tropical zones:

- Case of the Lobo watershed in the center-west of Côte d'Ivoire. Ivorian Journal of Science and Technology. 2012;19:136-157.
5. Kouassi AM, Kouamé KF, Saley MB, Biemi J. Application of the Mallet model to the study of the impacts of climate change on water resources in West Africa: Case of the N'Zi-Bandama watershed (Ivory Coast). Journal of Asian Scientific Research. 2013 ;3(2):214-228.
  6. Chareb YI Contribution to the methodology of flood protection studies: Application of the HEC-RAS and HEC-FDA models. Master's thesis, Oran Mohamed Boudiaf University of Science and Technology (Algeria) ; 2005;117.
  7. Hauhouot C. Analysis of the rain risk in precarious districts of Abidjan. Case study in Attécoubé. International Journal of Tropical Geology and Ecology. 2008;32: 75–82.
  8. OCHA (Office Coordination Humanitarian Affairs). Ivory Coast: Areas at risk of flooding and cholera; 2014. Available:www.unocha.org / Côte d'Ivoire
  9. Adopo KL. Characterization of the hydrosedimentary functioning of an estuarine environment in a tropical zone: Case of the mouth of the Comoé river in Grand Bassam (south-eastern Côte d'Ivoire). Doctoral thesis, UFR of earth sciences and mineral resources, University of Cocody (Abidjan, Ivory Coast). 2009;179 .
  10. Brida AB. Development of the hydro-climatic atlas of Côte d'Ivoire: Statistical study of stream flows and water balance. DEA thesis, UFR of Environmental Sciences and Management, Nangui Abrogoua University (Abidjan, Ivory Coast). 2005;117.
  11. Mohamed M, Abdelkader SBA. Analyse statistique et prévision des débits de crues dans le bassin versant de l'Oued Makerra (Ouest de l'Algérie). Researchgate. 2007;1-19.
  12. Chow VT. Open Channel Hydraulics. McGraw hill company, Illinois (USA). 1959 ;245.
  13. Soro GE. Statistical modeling of extreme rains in Côte d'Ivoire. Unique Doctoral Thesis, UFR des Sciences et Gestion de l'Environnement, Abobo-Adjamé University (Abidjan, Ivory Coast). 2011;172.
  14. Kasuri L. Modeling for ecosystem restoration hydrodynamic modeling of Yolo bypass using HEC-RAS. Master of sciences in civil engineering, University of California (USA). 2013;25p.
  15. Soualmia A, Gharbi M, Dartrus D, Masbernat L. Comparaison of 1D and 2D hydraulic model for floods simulation on the Medjerdariverin Tunisia. Journal Mater. 2016;7:3017-3026.
  16. Kouassi KL, Kouadio ZA, Kouame YM, Yao AB, Ouedé GB, Kouadio KP. Modeling of the influence of a threshold on the propagation of floods from the Davo river to the drinking water production station in Guéyo (côte d'Ivoire). University Jean Lorougnon Guédé, BP 150 Daloa, Côte d'Ivoire. International Journal of Innovation and Applied Studies. 2019;28(1);241-253. ISSN 2028-9324.
  17. Baptista M. Contribution to the study of the propagation of floods in hydrology. Doctoral thesis, National School of Bridges and Roads (Paris, France). 1990;292.
  18. Archambeau P. Contribution to the modeling of the genesis and propagation of floods and floods. Doctoral thesis, University of Liège (Belgium). 2006;419.
  19. Seck M. Flooding at the mouth of the Senegal River. DESS thesis, Inter-State School of Rural Equipment Engineers (Burkina Faso). 2004;70.
  20. Kouadio ZA. Land use dynamics and hydrological behavior: case of the coastal watersheds of Agnéby and Boubo (Ivory Coast). Doctoral thesis, UFR Environmental Sciences and Management, Nangui Abrogoua University (Abidjan, Ivory Coast). 2011;188.

© 2021 Kouassi et al.; This is an Open Access article distributed under the terms of the Creative Commons Attribution License (<http://creativecommons.org/licenses/by/4.0>), which permits unrestricted use, distribution, and reproduction in any medium, provided the original work is properly cited.

Peer-review history:

The peer review history for this paper can be accessed here:  
<http://www.sdiarticle4.com/review-history/64461>